

IMECE2005-81732

## MICRO-CANTILEVER BASED METROLOGY TOOL FOR FLOW CHARACTERIZATION OF LIQUID AND GASEOUS MICRO/NANOJETS

Jungchul Lee<sup>1</sup>, Kianoush Naeli<sup>2</sup>, Hanif Hunter<sup>1</sup>, John Berg<sup>1</sup>, Tanya Wright<sup>1</sup>, Christophe Courcimault<sup>2</sup>, Nisarga Naik<sup>2</sup>, Mark Allen<sup>2</sup>, Oliver Brand<sup>2</sup>, Ari Glezer<sup>1</sup>, and William King<sup>1</sup>

<sup>1</sup>Woodruff School of Mechanical Engineering, Georgia Institute of Technology, Atlanta, GA

<sup>2</sup>School of Electrical and Computer Engineering, Georgia Institute of Technology, Atlanta, GA

### ABSTRACT

This paper reports the development of MEMS metrology tools to characterize liquid and gaseous jets ejected from micro/nanofabricated nozzles. To date few highly local measurements have been made on micro/nanojets, due in part to the lack of characterization tools and techniques to investigate their characteristics. Atomic force microscope cantilevers are well-suited for interrogating these flows due to their high spatial and temporal resolution. In this work, cantilever sensors with either integrated heating elements or piezoresistive elements have been fabricated to measure thrust, velocity, and heat flux characteristics of micro/nanojets.

### KEYWORDS

Atomic Force Microscope, heated cantilever, piezoresistive cantilever, micro/nanojets, anemometry

### INTRODUCTION

Micro- and nanoscale jets have potential applications in drug delivery, micro surgery [1], inkjet printing, microelectronics cooling [2], and precision manufacturing [3]. While  $O(100 \sim 1000 \mu\text{m})$ -scale high-speed gaseous jets have been investigated as potential actuators for flow control applications, little work has been reported on free liquid and gaseous jets having characteristic scales that extend below  $10\mu\text{m}$ .

Atomic force microscope (AFM) cantilevers have become perhaps the most widely used transducer for sensing and actuating at the nanometer scale [4]. Micromachined silicon cantilever beams have been applied in liquid fluid flow volume sensing [5, 6] and highly sensitive piezoresistive cantilevers have been introduced for measuring air flow velocity in a small pipe [7]. Due to their high spatial and temporal resolution, micromachined cantilevers can be versatile tools for interrogating micro/nanojets. Liquid jets from microscale nozzle can be examined with optical diagnostic tools but liquid jets from much smaller nozzle or gaseous jets are difficult to visualize or characterize using those tools.

The cantilevers used to interrogate the micro/nanojets are of two types: cantilevers with integrated heating elements and piezoresistive cantilevers. The heated cantilevers were originally developed for data storage by Stanford [8] and IBM [9], but have recently been redesigned and fabricated at Georgia Tech to extend their functionality beyond data storage application (Fig.1 (a) and (d)). Both commercially available (Fig. 1 (b) from PSI) and fabricated piezoresistive cantilevers (Fig. 1 (c)) are introduced for deflection sensing since optical lever technique is difficult to be incorporated under the liquid jet environment. The piezoresistive cantilevers can measure deflection which can be correlated into thrust and velocity due to momentum transfer and detect mass of liquid droplets when the liquid sticks to the cantilever surface in a resonant mode.

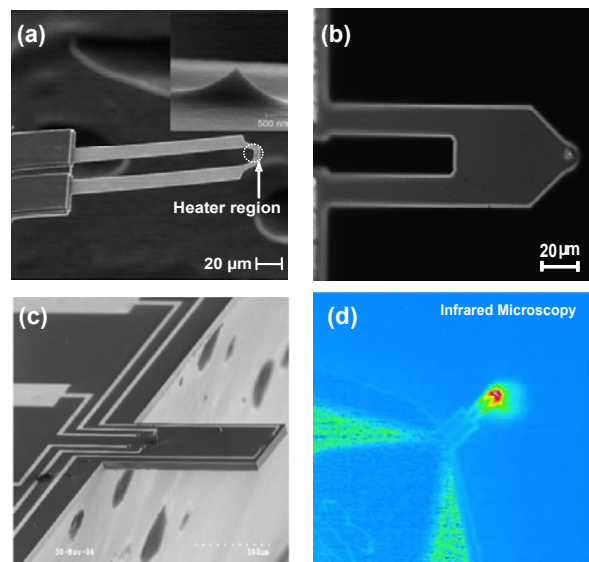


Figure 1. (a) SEM image of the fabricated heated cantilever (b) commercial Piezolever (c) fabricated piezoresistive cantilever (d) Infrared microscope image of the fabricated heated cantilever with electrical heating.

The heated cantilevers are expected to examine cooling capacity of micro/nanojets by heat transfer between heating element and jet environment and act as an anemometry which can measure velocity like a hot-wire.

This paper presents novel metrology application of AFM cantilevers to interrogate micro/nanojets flow. The jets are formed by micromachined silicon nozzles defined in the chip plane and laser drilled stainless nozzles connected to a small-scale pressurized reservoir. Liquid butane and propane and gaseous nitrogen jets ejected from 600 nm to 12  $\mu\text{m}$  diameter nozzles have been generated and characterized with the cantilever sensors.

## EXPERIMENT

Figure 2 shows the experimental setup which enables to switch two different types of cantilever sensors. The cantilevers and mount assembly and microfabricated nozzle and packing assembly are controlled by independent motorized 3-axis transverse stage. The flow field is illuminated using a double-pulse ND:Yag laser (532 nm) where the duration of the laser pulse is on the order of 5 nsec. Instantaneous images of the flow are captured using a PIV CCD camera having 1008 x 1018 pixels equipped with a high-magnification microscope lens. The lens system consists of a 50x infinity corrected microscope objective lens coupled with a 6.5x lens and 2x extension tube for a total maximum magnification of 228x. The smallest field of view measures 28  $\mu\text{m}$  on the side. Another camera-link CCD camera is equipped for alignment and inspection.

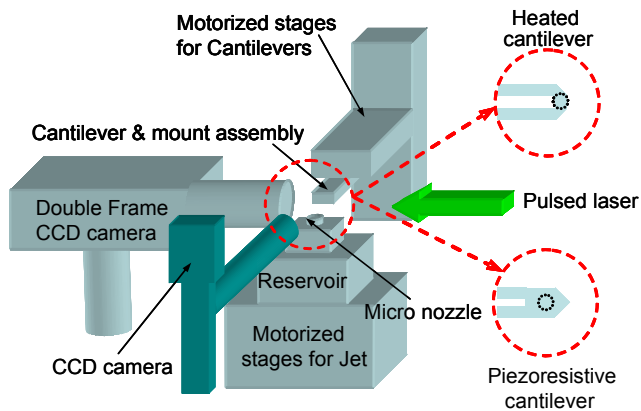


Figure 2. Experimental setup which enables to switch two different types of cantilever sensors.

The working liquids are propane and butane which have similar surface tension, but propane has a higher vapor pressure than butane. Figure 3 shows the constructed fluidic system suitable for the generation of high-speed submicron-scale jets. The maximum operating pressure of the present system is 34.5 MPa. In this system, nitrogen is used for pressurizing. Before the system is filled with the working liquid, it is first pressurized slightly above its vapor pressure using nitrogen, and then the liquid is pumped into the reservoir to the desired level. The system is then pressurized again to the desired driving pressure using nitrogen. The jet nozzle is directly connected to the reservoir and is designed to minimize volume

and the possibility of nitrogen pockets. When the working liquids are not introduced to the reservoir, gaseous nitrogen jet can be driven.

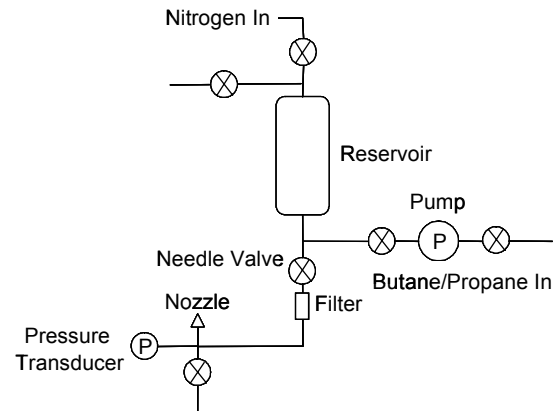


Figure 3. Fluidic system diagram.

Figure 4 shows the configuration of cantilever and microfabricated nozzle. Once the position of the nozzle and reservoir assembly fixed, the piezoresistive cantilever is brought close to the jets and scanned over the entire effective flow field. When the pre-calibrated piezoresistive cantilever bends up due to the jet, the deflection can be obtained using wheatstone bridge and differential amplifier. The heated cantilever needs to be stationary so that the heating element near its tip can be fully exposed to the jet environment continuously. Since the resistance change of the heated cantilever is much greater than that of the piezoresistive cantilever, measurement can be done with one additional resistor connected to the cantilever in series. Both cantilever types are powered by Keithley sourcemeter 2400 and monitored by Agilent 34401A multimeter. Both liquid and gaseous jets are tested by piezoresistive cantilever. However, the heated cantilever examines liquid jet only.

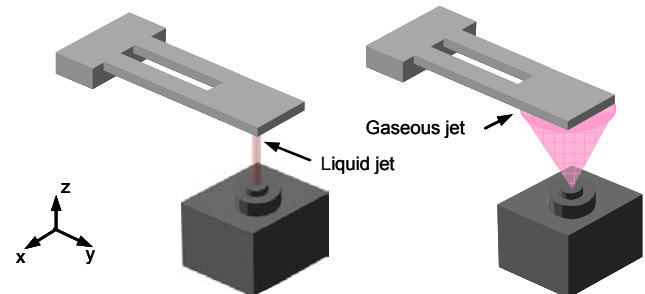


Figure 4. Configuration of nozzle and cantilever.

## RESULTS

Piezoresistive cantilevers are introduced first to estimate thrust and velocity of the micro/nanojets. The temperature of liquid butane and propane is much lower than ambient temperature but the temperature of nitrogen gas is close to the ambient. Since piezoresistive cantilevers are sensitive to deflection and temperature, they need to be calibrated for both applied deflection and environment temperature. Calibration setup is constructed using precise motorized micro-transverse and optical microscope. Figure 5 shows the calibration results of the piezoresistive cantilever with applied deflection. The voltage

read out increases linearly with cantilever deflection. Then, the cantilever is mounted in the cryostat to check the temperature dependency of the cantilever sensor.

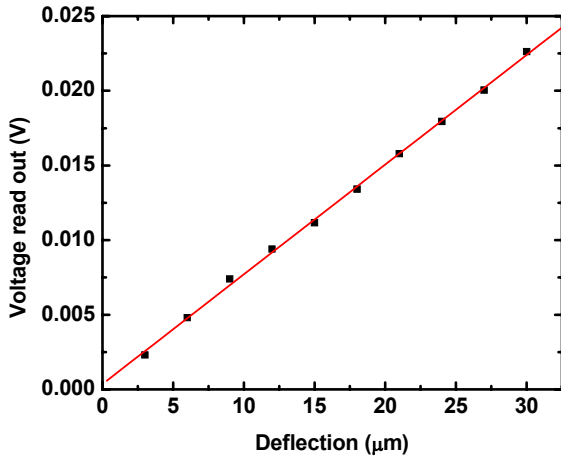


Figure 5. Voltage read out from wheatstone bridge with the cantilever deflection.

Figure 6 shows that the sensor read out changes in parabolic with the sensor temperature under the assumption of thermal equilibrium between cantilever and mounting stage in the cryostat. When the piezoresistive cantilevers are operated at lower or higher than ambient temperature, offset of the sensor read out should be compensated to estimate actual cantilever deflection.

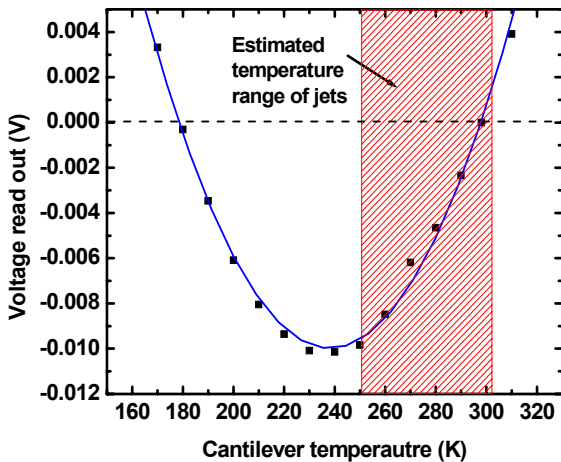


Figure 6. Voltage read out from wheatstone bridge at different cantilever temperature.

After the piezoresistive cantilever is calibrated, the cantilever is scanned over the effective flow field of the liquid and gaseous micro/nanojets. Figure 7 shows the piezoresistive cantilever is immersed in the liquid butane free jets from 12 μm diameter nozzle and bends up. The sensor read out data are recorded and processed to be converted into cantilever actual deflection using calibration results.

Figure 8 shows the measured cantilever deflection as the cantilever is traversed through liquid butane jets generated from

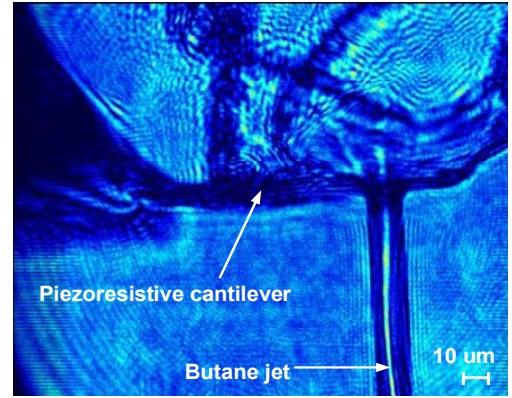


Figure 7. Piezoresistive cantilever bends up when the liquid butane jets hit the bottom surface of the cantilever.

a 6 μm microfabricated silicon nozzle with 130 μm separation between cantilever and nozzle. Each deflection curve has a plateau which indicates that the cantilever deflection is nearly constant once the jets are blocked completely by the cantilever and there is negligible torsional motion.

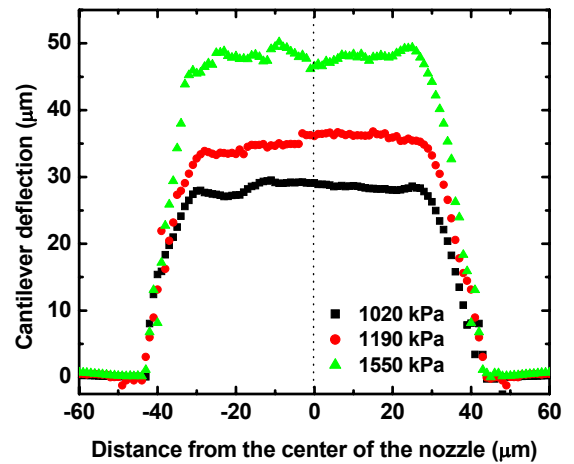


Figure 8. Deflection of the piezoresistive cantilever as the cantilever is traversed through liquid butane jets generated from a 6 μm diameter silicon nozzle with 130 μm separation between cantilever and nozzle.

When the liquid butane jets are aligned to the center of the cantilever in the scanning direction, the thrust ( $F$ ) of the jets can be obtained by the equation (1) with the assumption that the piezoresistive cantilever has constant rectangular cross-section from free end to base and experiences pure bending.

$$F = \frac{2L^3}{a^2(3L-a)}k\delta \quad (1)$$

where,  $L$ ,  $a$ ,  $\delta$ , and  $k$  are cantilever length, distance from the cantilever free end to the center of the jets, cantilever deflection, and spring constant, respectively [10]. Distance  $a$  is measured with PIV CCD camera and spring constant of the piezoresistive cantilever is obtained using AFM system before jet testing. Once the thrust is calculated, jet velocity ( $V$ ) can be estimated by the equation (2).

$$V = \sqrt{\frac{F}{\rho A_{\text{jet}}}} \quad (2)$$

where,  $F$ ,  $\rho$ , and  $A_{jet}$  are thrust, density of the liquid jets, and cross-sectional area of the jets, respectively [11].

Three assumptions are made to estimate jet velocity. First, the cross-section of the liquid jets is a perfect circle and diameter of the jets is measured using CCD camera. Second, the density of the liquid jets does not change much with driving pressure after the jets are ejected from the nozzle. The third assumption is that momentum of the jets is fully transferred to the cantilever. Jet velocities at different driving pressures are calculated by the equation (2) and compared with the data obtained using laser shadowgraphy as shown in the Fig. 9.

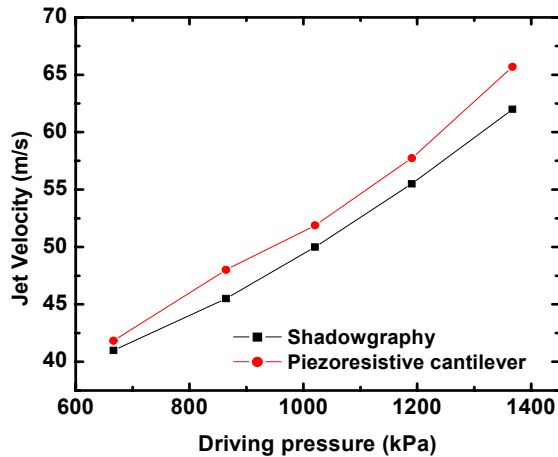


Figure 9. Measured jet velocity using piezoresistive cantilever and shadowgraphy.

The velocity data from piezoresistive cantilever show good agreement with the measured velocity using shadowgraphy image. Since piezoresistive sensing can detect nm/Å range deflection [12], the piezoresistive cantilever is sensitive enough to measure thrust and jet velocity from the nozzle of which diameter is much smaller than the wavelength of currently available laser while the optical diagnostic tools such as  $\mu$ -PIV and shadowgraphy struggle.

Gaseous micro/nanojets are also tested using the same fluidic system with the needle valve connected the working liquids supply closed. Figure 10 shows the measured cantilever deflection as the piezoresistive cantilever is traversed through gaseous nitrogen jets generated from a  $1 \mu\text{m}$  microfabricated silicon nozzle with  $27 \mu\text{m}$  separation between cantilever and nozzle. With different to the liquid jets, this deflection curves are almost symmetric and have a maximum deflection when the cantilever is aligned to the center of the nozzle. The effective flow field of gaseous jets is much larger than that of liquid jets even much smaller diameter nozzle is used. A conclusion can be drawn that the gaseous jets spread out while the cross-section of liquid jets is uniform as shown in the Fig. 4 even the gaseous jets can not be visualized. Figure 10 also shows the effective flow field of gaseous nitrogen jets does not change for driving pressure range from 1000 to 1500 psi.

Figure 11 shows the linear relationship between cantilever maximum deflection and driving pressure. Once the driving

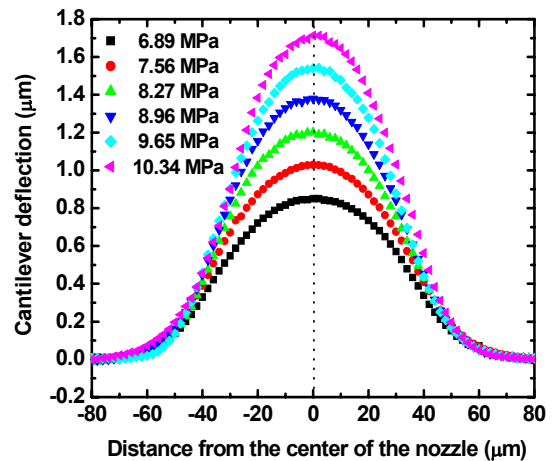


Figure 10. Deflection of the piezoresistive cantilever as the cantilever is traversed through gaseous nitrogen jets generated from a  $1 \mu\text{m}$  diameter silicon nozzle with  $27 \mu\text{m}$  separation between cantilever and nozzle.

pressure is fixed, the cantilever maximum deflection can be estimated. Currently, thrust and velocity estimation for gaseous jets can not be done since the interaction between the cantilever and gaseous jets is more complicated because the gaseous jets easily spread out and small portion of the jets have only vertical direction velocity component.

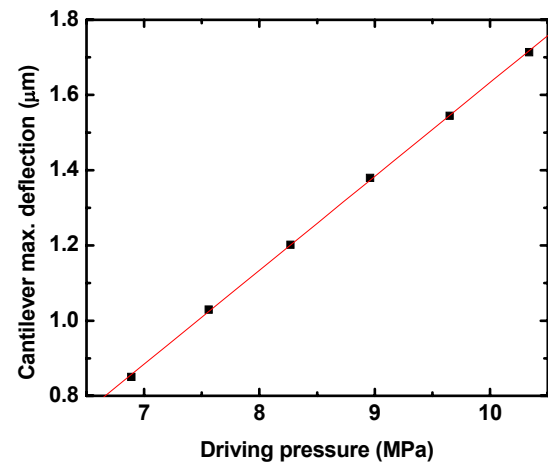


Figure 11. Linear relationship between cantilever maximum deflection and driving pressure.

The piezoresistive cantilever is switched with the heated cantilever which has integrated micro-heater near its tip to investigate cooling capacity of the liquid microjets and interaction between cantilever heater and liquid jets environment. The heated cantilever has positive temperature coefficient of resistance (TCR) at low temperature and negative TCR at high temperature [13]. Resistance of the heated cantilever is calibrated using infrared microscope at relatively low temperature where the cantilever has positive TCR and results are shown in the Fig. 12.

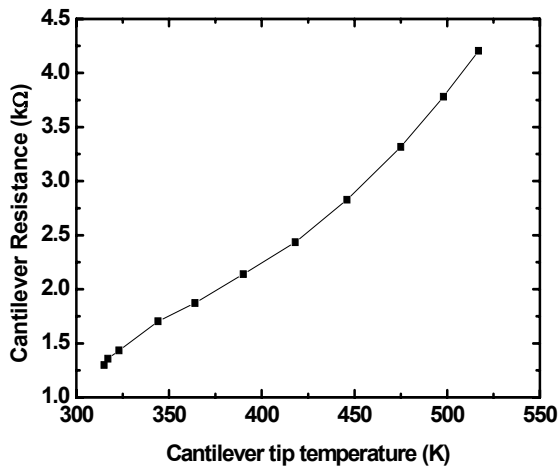


Figure 12. Heated cantilever electrical resistance as a function of temperature from infrared microscope.

After the heated cantilever is calibrated, the heater region of the cantilever is aligned to and impinged by the liquid microjets from 10  $\mu\text{m}$  diameter stainless nozzle. Figure 13 shows that resistance of the heated cantilever changes with the dissipated power in the cantilever with and without jet impingement. When liquid jets impinge the cantilever heater region, the cantilever can dissipate more power without significant heating than when the cantilever operates without jet impingement. Figure 13 also shows that there are discontinuities which indicate vaporization of liquid butane droplets at a critical power and this critical power increases as jet velocity increases. Liquid butane droplets form around the heated cantilever legs at power lower than the critical power; however, the droplets vaporize and disappear at higher power as shown in the Fig. 14. Before the liquid droplets vaporize, the cantilever looks almost fully surrounded by the cold liquid environment and resistance vs. power plots are independent of jet velocity. Once the droplets vaporize completely, the cantilever can dissipate more power at same electrical resistance as the jet velocity increases.

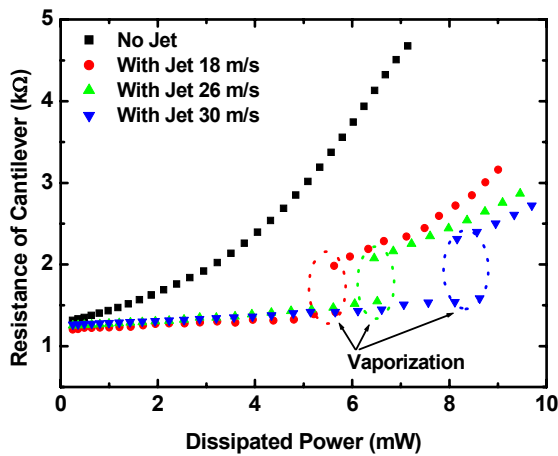


Figure 13. Resistance of heated cantilever as a function of dissipated power with and without additional cooling by liquid microjets.

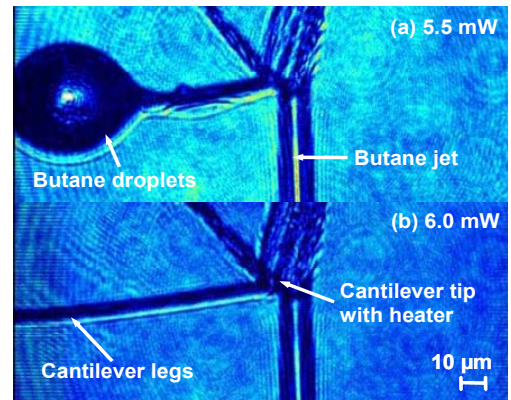


Figure 14. Liquid butane droplets form around the heated cantilever legs (top), the droplets vaporize and disappear at higher power (bottom). The measured jet velocity is 18 m/s.

Whereas similar analysis or operation to convention hot wire or hot film anemometry is not applicable right away, the heated cantilever can still measure velocity of liquid microjets by monitoring the critical power as shown in the Fig. 15.

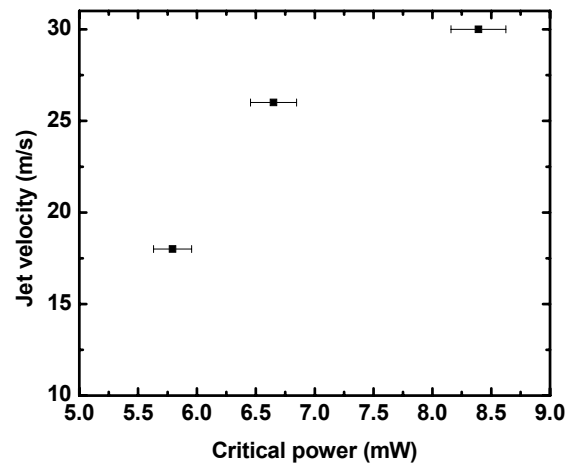


Figure 15. Jet velocity measured by monitoring the critical power of the heated cantilever.

## CONCLUSIONS

Liquid butane and gaseous nitrogen jets ejected from 600 nm to 12  $\mu\text{m}$  diameter nozzles have been generated and characterized with the two different cantilever sensors. The piezoresistive cantilever can measure thrusts ranging from 40 to 100  $\mu\text{N}$  and estimate jet velocities which agree to the shadowgraphy results within 6 % with the liquid microjets from a 6  $\mu\text{m}$  diameter nozzle. The piezoresistive can also investigate effective flow field, estimate how much the jets spread out – especially for gaseous jets-, and check whether the nozzle is clogged. Since the piezoresistive sensing can detect nm/ $\text{\AA}$  deflection, the piezoresistive cantilever can be well-suited for nanoscale jets characterization.

With the heated cantilever, local vaporization of liquid butane droplets and localized cooling capability of the liquid microjets

can be examined. There is a critical power which indicates vaporization of liquid butane droplets and increases with jet impinging velocity. Our results present the possibility of the cantilever metrology for interrogating liquid and gaseous micro/nanoscale jets.

## ACKNOWLEDGMENTS

The work was partially funded by an NSF-NIRT.

## REFERENCES

- [1] Fletcher, D. A. and Palanker, D. V., 2001, "Pulsed Liquid Microjet for Microsurgery," *Applied Physics Letters*, **78**(13), pp. 1933-1935.
- [2] Wang, E. N., Zhang, L., Jiang, L., Koo, J.-M., Maveety, J. G., Sanchez, E. A., Goodson, K. E., and Kenny, T. W., 2004, "Micromachined Jets for Liquid Impingement Cooling of VLSI Chips," *Journal of Microelectromechanical systems*, **13**(5), pp. 833-842.
- [3] Sibailly, O. D., Wagner, F. R., Mayor, L., and Richerzhagen, B., 2003, "High Precision Laser Processing of Sensitive Materials by Microjet," *Fourth International Symposium on Laser Precision Microfabrication*, **5063**, pp. 501-504.
- [4] Binnig, G., Despont, M., Drechsler, U., Häberle, W., Lutwyche, M., Vettiger, P., Mamin, H. J., Chui, B. W., and Kenny, T. W., 1999, "Ultrahigh-Density Atomic Force Microscopy Data Storage with Erase Capability," *Applied Physics Letters*, **76**, pp. 1329-1331.
- [5] Nishimoto, T., Shoji, S., and Esashi, M., 1994, "Buried Piezoresistive Sensors by Means of Mev Ion Implantation," *Sensors and Actuators A*, **43**, pp. 249-253.
- [6] Gass, V., VanderSchoot, B. H., and DeRooij, N. F., 1993, "Nanofluid Handling by Micro-Flow Sensor Based on Drag Force Measurement," *Proc. MEMS 93*(New York: IEEE), pp. 162-172.
- [7] Su, Y., Evans, A. G. R., Brunnschweiler, A., and Ensell, G., 2002, "Characterization of a Highly Sensitive Ultra-Thin Piezoresistive Silicon Cantilever Probe and Its Application in Gas Flow Velocity Sensing," *Journal of Micromechanics and Microengineering*, **12**, pp. 780-785.
- [8] Chui, B. W., Stowe, T. D., Ju, Y. S., Goodson, K. E., Kenny, T. W., Mamin, H. J., Terris, B. D., and Ried, R. P., 1998, "Low-Stiffness Silicon Cantilever with Integrated Heaters and Piezoresistive Sensors for High-Density Data Storage," *Journal of Microelectromechanical Systems*, **7**, pp. 69-78.
- [9] Vettiger, P., Cross, G., Despont, M., Drechsler, U., Duerig, U., Gotsmann, B., Haberle, W., Lantz, M., Rothuizen, H., Stutz, R., and Binnig, G., 2002, "The "Millipede"-Nanotechnology Entering Data Storage," *IEEE Transactions on Nanotechnology*, **1**, pp. 39-55.
- [10] Crandall, S. H., Dahl, N. C., and Lardner, T. J., *An Introduction to the Mechanics of Solids*, 2nd ed.
- [11] Munson, B. R., Young, D. F., and Okiishi, T. H., *Fundamentals of Fluid Mechanics*, 4th ed.
- [12] Yu, X., Thaysen, J., Hansen, O., and Bolsen, A., 2002, "Optimization of Sensitivity and Noise in Piezoresistive

Cantilevers," *Journal of Applied Physics*, **92**(10), pp. 6296-6301.

- [13] Lee, J., Wright, T. L., Abel, M., Sunden, E., Marchenkov, A., Graham, S., and King, W. P., 2005, "Characterization of Heated Atomic Force Microscope Cantilevers in Air and Vacuum," *Proceedings of ASME IPACK*.